Structure, dynamics, and phase transitions in the fullerene derivatives $C_{60}O$ and $C_{61}H_2$

C. Meingast, G. Roth, and L. Pintschovius
Forschungszentrum Karlsruhe-Technik und Umwelt, Institut für Nukleare Festkörperphysik, P.O. Box 3640, D-76021 Karlsruhe, Germany

R. H. Michel, C. Stoermer, and M. M. Kappes
Universität Karlsruhe, Institut für Physikalische Chemie II, D-76128 Karlsruhe, Germany

P. A. Heiney
Department of Physics, University of Pennsylvania, Philadelphia, Pennsylvania 19104

L. Brard, R. M. Strongin, and A. B. Smith III
Department of Chemistry, University of Pennsylvania, Philadelphia, Pennsylvania 19104
(Received 3 November 1995)

The effect of perturbing the icosohedral symmetry of C_{60} by the addition of the side groups -O and -CH_2 upon orientational order-disorder and glass transitions in solid C_{60} has been studied by a combination of high-resolution capacitance dilatometry and single-crystal x-ray and powder inelastic neutron scattering. Both fullerene derivatives $C_{60}O$ (epoxide) and $C_{61}H_2$ (6,5-annulene) are shown to undergo a sequence of transitions similar to that found in pure C_{60}, i.e., a first-order orientational ordering transition just below room temperature followed by an orientational glass transition at lower temperatures. Although the exact origin of the glass transition in $C_{61}H_2$ is unclear, the glass transition in $C_{60}O$ has the same origin as that in C_{60}, with a significantly higher degree of order due to a larger energy difference between pentagon and hexagon orientations. The dilatometric data at the glass transition indicate that, in contrast to C_{60}, the ground-state orientation of both $C_{60}O$ and $C_{61}H_2$ molecules is that with the smallest volume, also demonstrating a significant influence of the side groups upon the details of the structure. A possible explanation of these differences in terms of steric effects is proposed. [S0163-1829(96)04125-2]

I. INTRODUCTION

Crystalline C_{60} and other fullerene compounds continue to attract considerable attention due to their interesting solid-state properties. At high temperatures, pristine C_{60} is a prototypical *plastic crystal*; i.e., the molecules show dynamical orientational disorder, while their centers of mass form a well-ordered face-centered-cubic lattice.[1–3] At 260 K, C_{60} undergoes a structural phase transition where the molecules develop orientational order.[1–4] However, the low-temperature phase is not totally ordered, as each molecule can take on one of two energetically nearly equivalent orientations.[4,5] These two orientations are such that double bonds (short 6-6 bonds) of one molecule point toward pentagons (ground state) or hexagons (excited state) of adjacent molecules. As the temperature is lowered, more and more molecules take on the energetically favorable pentagon orientation. However, below 90 K the reorientational kinetics becomes extremely slow because of an energy barrier of ~250–300 meV between the two orientations, so that the remaining disorder is frozen in. This freezing-in process is seen quite prominently in thermal expansion measurements[6] and has many of the features of a conventional glass transition.[7]

This ''glass transition'' in C_{60} is unusual and has attracted considerable attention because it involves the conformational dynamics of a *single*, highly symmetric molecule, which interacts only weakly with its neighbors and results in particularly simple structural relaxation properties.[7] This is in contrast with multicomponent systems, such as KBr, or strongly linked network systems, such as silicate glasses, in which the relaxation is much more complex. Under these circumstances, it is instructive to ask what the effect would be of perturbing the symmetry of C_{60} and hindering its rotational dynamics by the addition of a side group such as -O or -CH_2. Surprisingly, previous structural studies[8–11] have already shown that both $C_{60}O$ and $C_{61}H_2$ undergo order-disorder phase transitions very similar to the one found in pure C_{60} and that, therefore, these modifications do *not* substantially affect the long-range crystalline order of these fullerene solids. Molecular dynamics calculations for $C_{60}O$ are in good agreement with these structural data.[12] Apparently, the extra O atom and the CH_2 group simply occupy the largest available space between molecules, and the structure is still determined largely by the C-C interactions. Up to now, it was not known whether these derivatives also have an orientational glass transition as found in pure C_{60}. In addition to the possible glass transition due to pentagon-hexagon disorder, it is also conceivable that there will be either an ordering transition or a glass transition due to the disorder of the side groups.

In this paper, we address the effect of these substituents on the glass transition and structure by a combination of high-resolution dilatometry and x-ray diffraction. As our previous studies on pure C_{60} have shown,[6] dilatometry is a powerful method not only for detecting a glass transition, but

also for extracting the activation energy of the relaxation process. In addition, we performed inelastic neutron scattering experiments on $C_{60}O$ to explore the rotational dynamics above and below T_s, from which we obtain information about the reorientational barriers.

The paper is organized as follows. The sample preparation and characterization are presented in Sec. II. Next, we discuss the single-crystal x-ray diffraction (XRD) results on $C_{60}O$ (Sec. III) followed by the dilatometry results of both $C_{60}O$ and $C_{61}H_2$ (Sec. IV). The neutron scattering data are shown in Sec. V, and finally a discussion and conclusions are given in Sec. VI. A short version of the dilatometry results has been published previously.[13]

II. SAMPLE PREPARATION

$C_{60}O$ was produced by ozonolysis of C_{60} in toluene solution.[14] In this procedure, ozone gas was bubbled through a solution of 30 mg C_{60} (Hoechst gold grade) and 50 ml toluene at room temperature with a flow rate of 20 ml/min for approximately 30 s. The solution was observed to rapidly change color from magenta to brown, coupled with the formation of some insoluble material. After standing for one night, the insoluble material was filtered off, and separation and purification was carried out on the soluble fraction of the reaction products via a semipreparative high performance liquid chromatography (HPLC) procedure. We made use of a HPLC system already described elsewhere[15] equipped with a Nucleosil-5-PAH column (10 mm×250 mm, Macherey-Nagel), which provides fast two-cycle separation. For this column, high throughputs and loading were obtained with a three-component eluent (60% toluene, 30% hexane, 10% dichloromethane at 5 ml/min). After the second cycle, the purity was checked to be >99% by HPLC analysis at 330 nm assuming similar extinction coefficients of $C_{60}O$ and $C_{60}O_x$ ($x \geq 2$). The solution was stored at 8 °C in toluene under air until use. Single crystals of $C_{60}O$ (100–300 μm) for x-ray and dilatometry investigations were grown from both toluene and benzene solutions. Details of the crystal quality will be given in Sec. III. The $C_{61}H_2$ was prepared and purified by treating a C_{60} toluene solution with ethereal diazomethane and drying under vacuum, as described previously.[9] No residual C_{60} or toluene could be detected by chromotography or infrared reflectance (we estimate that there is less than 1% C_{60} in the sample), and differential scanning calorimetry showed a sharp peak with an onset at 290 K, indicating a high degree of purity. The resulting powder was pressed into a 4 mm×2 mm pellet for the dilatometry measurements.

III. SINGLE-CRYSTAL X-RAY DIFFRACTION OF $C_{60}O$

Several single crystals of $C_{60}O$ were examined with a four-circle diffractometer using Mo Kα radiation and a graphite monochromator. Full data sets were taken at 296, 260, 190, and 120 K. At 296 K, the symmetry is $Fm3m$ and the data look very similar to those of pure C_{60} at room temperature, where, to a very good approximation, they are described by a homogenous hollow sphere. We find no clear evidence from difference Fourier synthesis for O occupation of octahedral or tetrahedral voids in the high-T phase, as suggested by the powder data.[18]

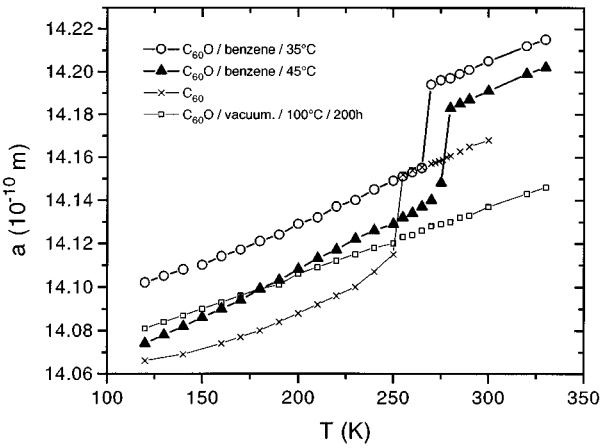

FIG. 1. Lattice parameter vs temperature from single-crystal x-ray diffraction for several different $C_{60}O$ crystals grown from a benzene solution. Also shown are the data for pure C_{60} and an annealed sample of $C_{60}O$, which shows no phase transition (see text for details). The uncertainties in a are about the size of the symbols.

Figure 1 shows the lattice parameters versus temperature for several $C_{60}O$ crystals (C_{60} data are also plotted). Noticeable is a sharp decrease in the lattice parameter of comparable size as found in pure C_{60}, indicating a similar kind of phase transition. The transition temperature (midpoint) varies between 267 and 277 K and appears to inversely correlate with the value of the lattice parameter above the transition. This effect may be attributed to a small amount of solvent being incorporated into the crystals, and the crystal with the highest transition temperature presumably has the least amount of solvent. The small size of the crystals prevented us from a quantitative analysis of solvent impurities.

The low-temperature phase has $Pa3$ symmetry, in agreement with the results of a powder diffraction study.[8] The crystals were found to be merohedrally twinned like crystals of pure C_{60}. There is clear evidence that the majority of the $C_{60}O$ molecules occupy the pentagon orientation like in pure C_{60}. On the other hand, it is not possible to identify the minority orientation from Fourier-difference-synthesis. However, a refinement using the pentagon and hexagon orientations gives reasonable results. Figure 2 shows that the qualitative dependence of the fraction of pentagon orientations, f_p, above 100 K is similar to that in C_{60}; f_p is higher at any given temperature, but f_p decreases with increasing temperature and a curve interpolated through the data points has positive curvature. Also, like C_{60}, the data point at 20 K (from Ref. 8) is clearly out of line with the other points at higher temperature. A simple two-state model $f_p = 1 - 1/[e^{\Delta/kT} + 1]$, with an energy difference Δ of $\sim$20 meV (dashed line in Fig. 2), provides a reasonable description of the data above 100 K. Note that this energy difference is significantly larger than in pure C_{60} ($\sim$11 meV, dotted line in Fig. 2). If we provisionally assume from the similarity of the low- and high-temperature data that C_{60} has a glass transition similar to that in C_{60}, we can estimate the glass-transition temperature by extrapolating the low- and high-temperature data, as shown by the solid lines in Fig. 2. This suggests that if there is a glass transition it is shifted to about 100 K in

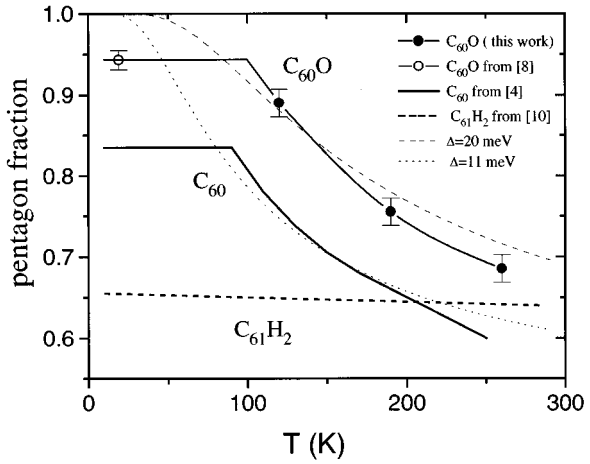

FIG. 2. Fraction of majority (pentagon) orientation vs temperature for $C_{60}O$ as determined from x-ray analysis (the 20 K data point was obtained from Ref. 8). The dashed and dotted lines are the equilibrium fractions for a two-level system with an energy difference of 20 and 11 meV, respectively. Also plotted are the data for pure C_{60} (Ref. 4) and for $C_{61}H_2$ (Ref. 10).

$C_{60}O$. Our dilatometry results (Sec. IV) confirm that this is indeed the case.

The positions of the O atoms found by difference-Fourier synthesis are the same as those proposed on the basis of powder data.[8] All short bonds pointing more or less into voids are partially occupied. The high crystal symmetry ($Pa3$) and low molecular symmetry ($mm2$ [C_{2v}]) lead to statistical occupation by the oxygen atom of multiple sites on the C_{60} shell,[8] and the apparent bond lengths result from a superposition of epoxy and nonepoxy bonds. This has as a consequence that no useful information can be obtained on the bridged C-C and C-O bond lengths.[16]

Unfortunately, it was not possible to obtain much more information from the single-crystal diffraction data than had already been obtained from powder measurements,[8] probably for the following reasons. First, as seen in Fig. 1, both the lattice parameters and transitions temperatures of the $C_{60}O$ crystals depend on the growth conditions, suggesting that some solvent is being incorporated into the crystals. In contrast to C_{60}, $C_{60}O$ cannot be grown by sublimation due to the low temperature stability of the $C_{60}O$ molecule, and solvent-free crystals can, therefore, not be made using this technique. The second possible reason for the unsatisfying single-crystal diffraction results may be directly related to the thermal instability of $C_{60}O$. We heated one of the $C_{60}O$ single crystals up to 100 °C under vacuum for several days to drive off possible residual solvent. This resulted in the complete suppression of the order-disorder phase transition and a lowering of the lattice parameter at 300 K as seen in Fig. 1. The symmetry was $Fm3m$ in the whole temperature range from 300 to 120 K, and dilatometry showed no transition between 10 and 310 K. We speculate that what happens is that a significant fraction of the $C_{60}O$ molecules forms $(C_{60}O)_n$ by fusing $C_{60}O$ molecules. $C_{60}O$ has recently been shown to react with C_{60} to form a furan structure $C_{120}O$.[17,18] $C_{120}O$ is expected to fit nicely into the cubic lattice, because quantum chemical calculations predict a furane-type bonding and a center-to-center molecular distance of 9.9 Å,[19] which is very similar to the center-to-center distance of crystalline $C_{60}O$. This is confirmed by recent C-NMR characterization of the isolated species $C_{120}O$.[18] Of course, the symmetry of $C_{120}O$ or $(C_{60}O)_n$ is incompatible with the cubic space-group symmetry, and, presumably, even a small fraction of $(C_{60}O)_n$ will lead to frustration of the order-disorder transition. It is possible that even the as-grown crystals already contain a very small percentage of $(C_{60}O)_n$, which would further complicate the interpretation of the single-crystal x-ray data.

IV. THERMAL EXPANSION OF $C_{60}O$ AND $C_{61}H_2$

The thermal expansion was measured with a high-resolution capacitance dilatometer capable of measuring length changes as small as 0.1 Å. The systematic errors in the expansion measurements, which are largely determined by the uncertainty in the length of the sample, are about $\pm 10\%$ and $\pm 2\%$ for $C_{60}O$ and $C_{61}H_2$, respectively. The measurements were made both upon cooling and heating at constant rates of the order of 1–20 mK/s. The inset in Fig. 3(a) shows the relative length changes $(\Delta L/L_{290\ \mathrm{K}})$ of several solution-grown $C_{60}O$ crystals around the order-disorder transition. For comparison, the data from a sublimation-grown C_{60} crystal[6] are also shown (dashed curve). Noticeable is that T_s of the transition varies between ~273 and 285 K for $C_{60}O$, as was already discussed in the previous section. In the following, we concentrate on the data of crystal 3 grown in toluene, which we believe to have the highest quality of the three as the transition is sharpest and T_s is highest.

The relative thermal expansion and corresponding expansivity, $\alpha(T) = 1/L\ dL/dT$, of this $C_{60}O$ crystal are shown in Figs. 3(a) and 3(b), respectively. Again for comparison, the data for pure C_{60} are also plotted. The total expansion of $C_{60}O$ between 10 and 300 K agrees quite well with the values determined by x rays[8] and is slightly larger than for pure C_{60} (we were unable to measure the expansion below 70 K due to a technical problem and have assumed that the expansion of $C_{60}O$ and C_{60} are the same below 70 K). The behavior of the expansivity of $C_{60}O$ and C_{60} at T_s is very similar, both curves exhibit significant precursors below the transition, which in this kind of plot makes the curve appear to have a λ shape. Above the transition, α of $C_{60}O$ is nearly 2 times as large as that for pure C_{60}. A possible reason for this is that as the temperature increases the O atoms spend on average less time in interstitial sites and more time between these sites; this is expected to result in an increase of the lattice parameter or larger thermal expansivity. The orientational glass transition, which in the data for pure C_{60} appears as a change of slope near 90 K,[4,6] seems to be absent in the $C_{60}O$ data. However, a closer inspection of the expansivity data in Fig. 3(b) shows a small anomaly in $\alpha(T)$ around 100 K. The other crystals investigated also showed this anomaly, and, as discussed in more detail below, this transition is indicative of a glass transition. We also observed small anomalies at 150 and 200 K in some of the crystals, but were unable to identify the nature of these.

A glass transition can be identified by performing measurements on different time scales, since glass transitions are of purely kinetic origin. The time scale in our dilatometry experiment is easily changed by making measurements at different cooling and heating rates. Figure 3(c) shows the

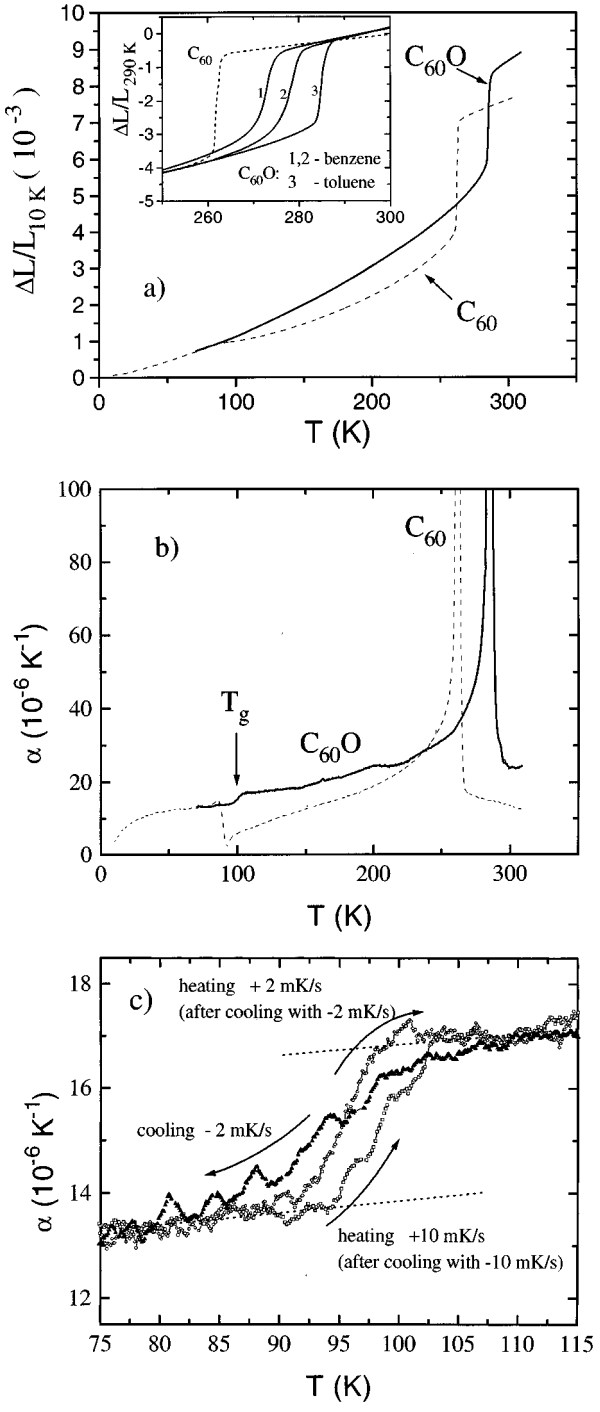

FIG. 3. Dilatometry data of a $C_{60}O$ single crystal. (a) Linear thermal expansion and (b) expansivity [$\alpha(T)=1/L\ dL/dT$]. For comparison the data from a single crystal of pristine C_{60} (dashed lines, from Ref. 6) are also shown. The inset in (a) shows the expansion behavior around T_s for several $C_{60}O$ crystals. (c) Details of the expansivity around the glass transition (see text for details). The apparently regular variation (peak and valley) of the cooling curve data in (c) is due to experimental noise.

details of expansivity near 100 K upon cooling and heating at a rate of 2 mK/s and upon heating at rate of 10 mK/s (after cooling also at 10 mK/s). These curves exhibit the typical signs of a kinetic transition, i.e., a hysteresis between cooling and heating curves (± 2 mK/s data) and a shifting of the

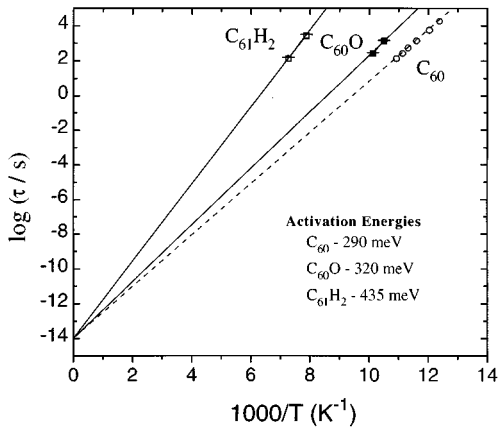

FIG. 4. Arrhenius plot of the relaxation times determined from dilatometry (see text for details). Data for pure C_{60} are taken from Ref. 6.

transition temperature to higher temperatures for larger cooling (heating) rates ($+2$ vs $+10$ mK/s data). The glass transition temperature T_g is increased by about 8 K relative to that in pure C_{60} [for the same cooling (heating) rates]. What is quite surprising is that the sign of the expansivity change at T_g is opposite to that in C_{60}; i.e., for $C_{60}O$, $\alpha(T)$ increases, rather than decreases, above T_g. A possible explanation of this behavior will be presented later. In C_{60} the relaxation time $\tau(T)$ is, to a good approximation, given by a simple Arrhenius law

$$\tau(T)=\frac{1}{\nu}\,e^{E_a/k_BT},$$

where $\nu\approx 10^{14}\ s^{-1}$ is an attempt frequency and $E_a\approx 290$ meV the activation energy.[6,7] The relaxation times for $C_{60}O$ can be obtained from the data in Fig. 3 by fitting the curves with a simple model.[6] The results are plotted in Fig. 4. The data do not cover a sufficiently large time interval in order to accurately determine both ν and E_a, and we have, therefore, fixed ν at $10^{14}\ s^{-1}$, which we believe is a reasonable assumption. In this way we obtain $E_a=320$ meV for $C_{60}O$, which is 11% higher than for pure C_{60}.

The thermal expansion data for $C_{61}H_2$ are presented in Fig. 5. Since these measurements were made on a pressed-powder pellet and not a single-crystalline sample, we also show, for comparison, the data of a pressed-powder pellet of pure C_{60}.[20] As can be seen from the C_{60} data, the pellet pressing process lowers and broadens the order-disorder transition and also reduces the size of the expansivity anomaly at the glass transition. This is presumably due to a large density of stacking faults generated during the nonuniform pressure treatment, which interferes with the collective nature of the order-disorder transition. The same features are seen in the $C_{61}H_2$ data. The order-disorder transition, which has an onset (from high T) near 300 K, is significantly broadened by $\sim$50 K. Differential scanning calorimetry measurements before and after the pellet pressing also clearly show that the transition is broadened by the pressing. Nevertheless, the integrated length change at the transition [$\sim$0.29% as indicated by dotted lines in Fig. 5(a)] is close to what is found in both pure C_{60} and $C_{60}O$. As in $C_{60}O$, the total ex-

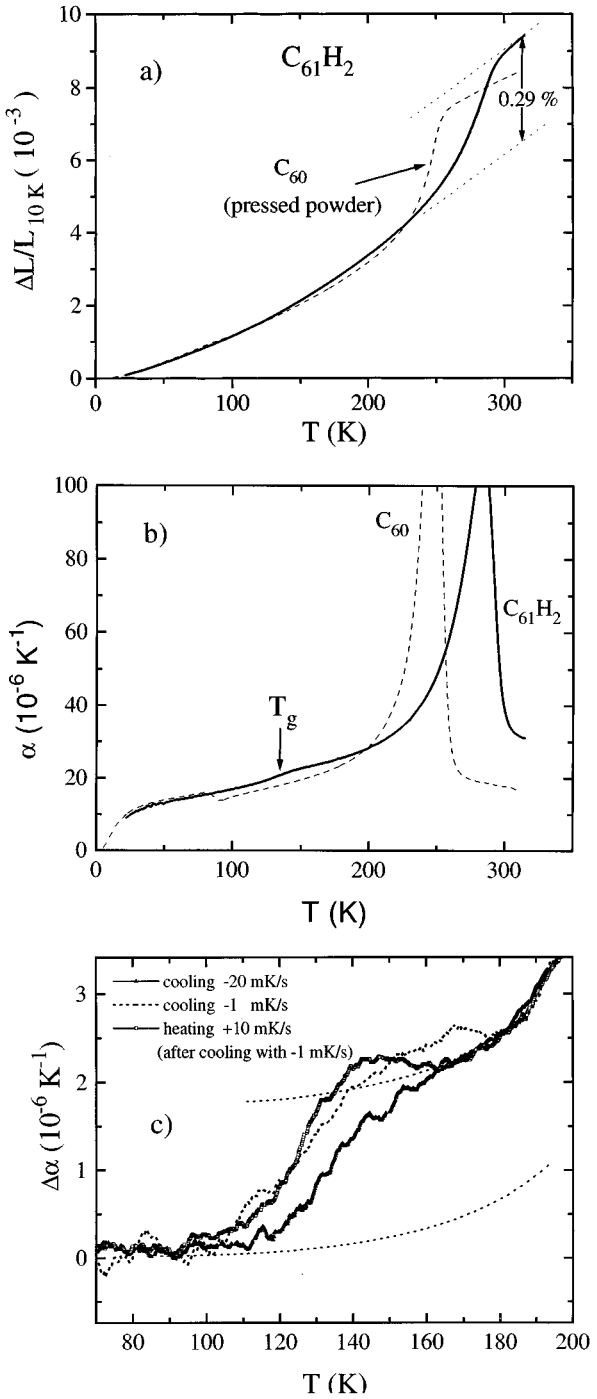

FIG. 5. Dilatometry data of a pressed pellet of $C_{61}H_2$. (a) Linear thermal expansion and (b) expansivity $[\alpha(T)=1/L\ dL/dT]$. (c) Details of the expansivity around the glass transition (see text for details). For comparison, expansion data of a pressed pellet of C_{60} (dotted lines) are also shown and indicate that pressing broadens the high-T transition and reduces the size of the glass transition anomaly (from Ref. 20).

pansion of $C_{61}H_2$ between 10 and 300 K is slightly larger than for pure C_{60}, and $\alpha(T>T_s)$ is roughly twice that of C_{60}. Evident in Fig. 5(b) is a small anomaly in $\alpha(T)$ near 130 K, which is shown in more detail in Fig. 5(c). A linear term fit to the data below the transition has been subtracted in order to make the anomaly clearer. Again, measurements performed at different cooling (heating) rates clearly demonstrate that this is a glass transition. The two cooling curves (-1 and -20 mK/s) are shifted relative to each other by about 10 K. There is only a very small hysteresis between cooling and heating curves, and the transition is quite broad ($\sim$50 K). Simulations of these data with the simple relaxation model[6] indicate that both of these features can be qualitatively explained if one includes a broad distribution of relaxation times. The average relaxation times obtained from these curves are plotted in Fig. 4. Again, using a fixed $\nu=10^{14}$ s^{-1}, we find an $E_a=435$ meV for $C_{61}H_2$, which is $\sim$50% higher than in C_{60}. As in $C_{60}O$, α increases above T_g in $C_{61}H_2$. There is no evidence for any further transition between 10 and 320 K in the expansivity data.

V. INELASTIC NEUTRON SCATTERING EXPERIMENTS ON $C_{60}O$

Inelastic neutron scattering experiments of powder samples are usually performed on samples with masses of one to several grams. For our investigations of $C_{60}O$, however, only a much smaller quantity was available, i.e., 5 mg. As a consequence, the investigations were restricted to low-energy transfers associated with the rotational dynamics.

The experiments were performed on the 2-T triple-axis spectrometer located at the ORPHEE reactor, Saclay, using horizontally and vertically focusing pyrolithic graphite crystals as monochromator and analyzer, respectively. The final energy was fixed to $E_f=14.7$ meV, and a pyrolithic graphite filter was placed in the scattered beam to suppress higher-order contamination. The energy resolution was between 0.8 meV ($\hbar\omega=0$) and 1 meV ($\hbar\omega=4$ meV). The accessible Q range was $Q\lesssim 4.8$ Å^{-1}. The temperature was varied between $T=70$ and 275 K.

Spectra taken below and just above T_s are shown in Fig. 6(a). The momentum transfer chosen was $Q=3.4$ Å^{-1} in order to maximize the scattering contributions associated with the rotational degrees of freedom. When choosing this particular momentum transfer, we assumed that the Q dependence of the scattering of $C_{60}O$ is similar to that of pure C_{60},[21,22] an assumption which is fully consistent with further measurements at different Q values. Above T_s there is a broad quasielastic feature centered at zero energy characteristic of rapid diffusive motion (we attribute the sharp component at $E=0$ to scattering from the sample holder). At $T=200$ K, two differences are apparent: First, the sharp component centered at $E=0$ increases, attributable to a freezing of orientational disorder. Second, a peak is observed at $E\sim 2.7$ meV, which we assign to hindered rotational motion, i.e., librations.

Very similar phenomena were observed on pure C_{60},[21,22] as well as on $C_{61}H_2$.[11] When trying to make a more quantitative comparison, one has to bear in mind that interpretation of neutron spectra like those shown in Fig. 6(a) is not straightforward as the scattering contains contributions not only from librational phonons, but also from translational ones, from muliphonons, and, of course, a background. What makes a comparison of peak positions as that shown in Fig. 6(b) defensible is the fact that the spectra for all the compounds in question were obtained under similar conditions. The comparison indicates that the orientational potential in

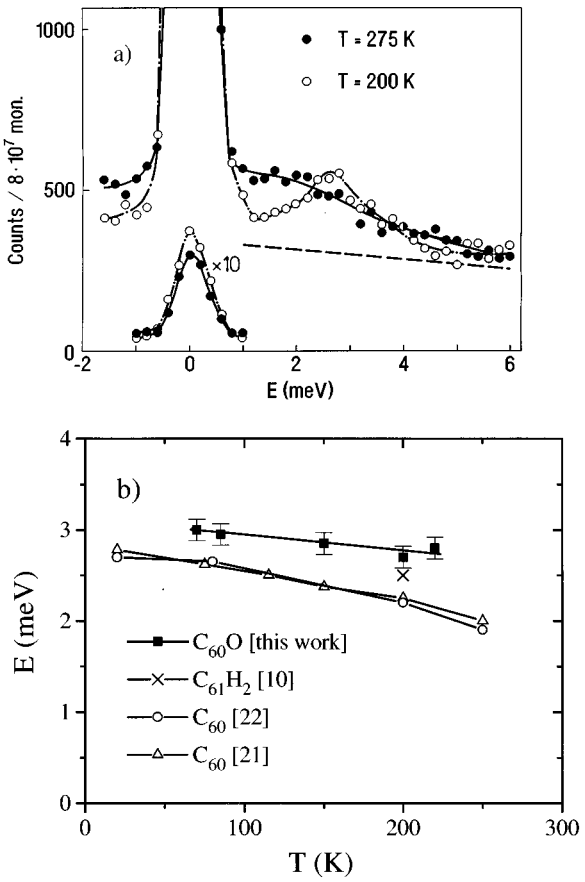

FIG. 6. (a) Inelastic neutron scattering spectra of polycrystalline $C_{60}O$ above and below T_s. (b) Comparison of average librational energies for $C_{60}O$, C_{60}, and $C_{61}H_2$ (see text for details).

$C_{60}O$ is significantly stiffer than in pure C_{60}, presumably due to the steric hindrance produced by the O atom.

VI. DISCUSSION AND CONCLUSIONS

The above results indicate that, qualitatively speaking, crystalline C_{60}, $C_{60}O$ (epoxide), and $C_{61}H_2$ (6,5-annulene) all behave very similarly. All undergo an orientational ordering transition just below room temperature and then an orientational glass transition between 90 and 140 K. Both the ordering and glass transitions in the derivatives are shifted to higher temperatures, which is most probably due to the higher reorientational potential barrier, as found in both the dilatometric and inelastic neutron data [see Figs. 4 and 6(b)]. However, distinct differences also exist between the three materials, which cannot be explained by just an increase in barrier height. The pentagon fraction for $C_{60}O$ exhibits a similar temperature dependence as found in C_{60}, but is significantly higher. For $C_{61}H_2$ this fraction appears to be temperature independent,[10] possibly indicating that the glass transition in $C_{61}H_2$ has a different origin than in pure C_{60}. Also, the expansivities increase above the glass transitions in both $C_{60}O$ and $C_{61}H_2$, whereas it decreases in pure C_{60}. In the following we discuss these similarities and differences in more detail.

The fact that the pentagon fraction for $C_{60}O$ increases as the temperature decreases is a strong indication that the glass transition observed near 100 K is due to the freezing in of the pentagon-hexagon disorder, just as in pure C_{60}. The reorientational barrier height, or activation energy, determined from dilatometry is only slightly larger (11%) than in pure C_{60}, suggesting that the reorientational jump mechanism is also similar for both $C_{60}O$ and C_{60}. For C_{60}, 42° jumps around $\langle 110 \rangle$ axes[2] have been suggested as having the smallest barrier height. A simple geometrical consideration shows that these same jumps are also possible in $C_{60}O$ even for the case that the O atom remains in a particular tetrahedral or octahedral site.

One can also roughly estimate the increase in reorientational barrier height from the increase in librational energy [see Fig. 6(b)] if one assumes a simple sinusoidal potential,[2] and this gives a barrier height increase of about 30%, which is significantly larger than the value derived from our dilatometry results. This difference can be understood when considering the molecular dynamics simulations of Cheng and Klein[12] which showed that the reorientational potential in $C_{60}O$ is more anisotropic than in pure C_{60}. In particular, the potential in which an O atom remains in a particular interstitial site was found to have a much smaller barrier than one for which the O atom changes sites.[12] Because the increase in barrier height derived from dilatometry is significantly smaller than the average one derived from our neutron study, this is also consistent with a reorientational mechanism at the glass transition where the O atom remains in a particular interstitial site.

What differentiates $C_{60}O$ from pure C_{60} is the higher pentagon order and the change in sign of the expansivity anomaly at the glass transition, both of which we believe are related to simple steric effects. Since the orientations of the molecules are governed by the $Pa3$ structure, the steric hindrance for an O atom sitting in a particular interstitial site will be different for the pentagon and hexagon orientations. We have tried to address the question of how well the O and CH_2 units fit into the interstitial sites by simply rotating rotating the central molecule in a three-dimensional (3D) model from pentagon to hexagon orientations and qualitatively assessing how well the adducts fit into the different sites. Our qualitative result is that the pentagon orientation in $C_{60}O$ is less disturbed by the steric hindrance,[23] which is expected to have several consequences. First, the energy difference between pentagon and hexagon orientations should increase, resulting in a higher pentagon fraction at low temperatures, as is observed (see Fig. 2). Also, the effective volume of the hexagon orientation should be increased more than that of the pentagon one. Our expansivity results suggest that this steric effect more than cancels the ~1% greater volume of the pentagon orientation (relative to the hexagon one) seen in pure C_{60} (Ref. 6) and actually results in a slightly smaller volume for the pentagon orientation. Of course, more detailed calculations of the importance of the steric effects in $C_{60}O$ would be of great value.

For $C_{61}H_2$ things appear to be quite different. Here the increase in reorientational barrier height from dilatometry (~50%) is actually larger than that deduced from the neutron data (~25%),[10] suggesting a much different jump mechanism at the glass transition than in C_{60} and $C_{60}O$. This is in accord with the fact that it is not possible to go from a hexagon to a pentagon orientation via 42° jumps in $C_{61}H_2$ with the methylene group remaining in an interstitial site. This

difference between $C_{61}H_2$ and $C_{60}O$ is due to the lower symmetry of the $C_{61}H_2$ molecule (the methylene group is attached to a 6-5 bond, whereas the O is attached to a 6-6 bond). A rotation of ~150° about an axis parallel to a [100] direction has been suggested as a possible way to go from one orientation to the other,[10] for which the potential is, however, expected to be much larger than for the simple 42° rotation and also contain several other minima. The real path a molecule takes between pentagon and hexagon orientations probably involves several small jumps around different axes and also significant residence in local minima. Thus one expects a distribution of barrier heights, some of which may be quite high, for this reorientation process. This may explain both the quite broad glass transition and the large barrier height we extract from the dilatometry measurements.

The only problem with the above interpretation is that the pentagon fraction, as determined from neutron data, shows little or no temperature dependence.[10] The magnitude of the anomaly in the expansivity at the glass transition, which is quite small, is proportional to the temperature derivative of the pentagon fraction in the simple model for C_{60},[6] and it may be possible that there exists a small temperature dependence, which has gone undetected in the neutron experiment. In this case the origin of the glass transition would also be due to pentagon-hexagon disorder. Alternative explanations of the glass transition in $C_{61}H_2$ are (1) that it is due to reorientation between some other orientations of the C_{60} cage or (2) that it is due to a rearrangement of the CH_2 groups in the available interstitial sites such that the C_{60} cage ends up in an equivalent orientation. Neumann *et al.* found evidence for two different hexagon orientations,[10] which differ in the position of the CH_2 group. Possibly, the relative fractions of these two different hexagon orientations are temperature dependent, thereby leading to glassy behavior.

As in $C_{60}O$, the expansivity of $C_{61}H_2$ increases above T_g, implying that the ground state has a smaller volume than the energetically less favorable state. This is actually what one usually finds for glass transitions, and maybe the behavior of C_{60} should be viewed as being anomalous, because here the energetically more favorable pentagon orientation has a larger effective volume than the less favorable hexagon orientation.

In conclusion, the structure and dynamics of the C_{60} derivatives $C_{60}O$ and $C_{61}H_2$ have been investigated with XRD, high-resolution dilatometry, and inelastic neutron scattering. To first order, the O and methylene groups only provide a steric hindrance to reorientation and the interesting physics (order-disorder transition and orientational glass transition) remains qualitatively unchanged. However, the details of the glass transition are strongly affected by the molecular additions. Especially, for $C_{61}H_2$ it remains unclear if this transition has the same origin as in pure C_{60}.

ACKNOWLEDGMENTS

M.M.K. acknowledges the support of the Bundesministerium für Bildung und Forschung (BMBF). Research at the University of Pennsylvania was supported in part by National Science Foundation Grant No. DMR-MRL-92-20668; acknowledgement is also made to the Donors of the Petroleum Research Fund, administered by the American Chemical Society, for partial support of this research.

[1] P. A. Heiney, J. Phys. Chem. Solids **53**, 1333 (1992).

[2] J. D. Axe, S. C. Moss, and D. A. Neumann, in *Structure and Dynamics of Crystalline C_{60}*, Solid State Physics, Vol 48, edited by H. Ehrenreich and F. Spaepen (Academic, New York, 1994).

[3] P. A. Heiney, J. E. Fischer, A. R. McGhie, W. J. Romanov, A. M. Denenstein, J. P. McCauley, Jr., A. B. Smith III, and D. E. Cox, Phys. Rev. Lett. **66**, 2911 (1991).

[4] W. I. F. David, R. M. Ibberson, T. J. S. Dennis, J. P. Hare, and K. Prassides, Europhys. Lett. **18**, 219 (1992).

[5] H. B. Bürgi, E. Blanc, D. Schwarzenbach, W. Liu, Y. Lu, M. M. Kappes, and J. A. Ibers, Angew. Chem. **104**, 667 (1992).

[6] F. Gugenberger, R. Heid, C. Meingast, P. Adelmann, M. Braun, H. Wühl, M. Haluska, and H. Kuzmany, Phys. Rev. Lett. **69**, 3774 (1992).

[7] C. Meingast and F. Gugenberger, Mod. Phys. Lett. B **7**, 1703 (1993).

[8] G. B. M. Vaughan, P. A. Heiney, D. E. Cox, A. R. McGhie, D. R. Jones, R. M. Strongin, M. A. Cichy, and A. B. Smith III, Chem. Phys. **168**, 185 (1992).

[9] A. N. Lommen, P. A. Heiney, G. B. M. Vaughan, P. W. Stephens, D. Liu, D. Li, A. L. Smith, A. R. McGhie, R. M. Strongin, L. Brard, and A. B. Smith III, Phys. Rev. B **49**, 12 572 (1994).

[10] D. A. Neumann, Q. Huang, J. R. D. Copley, J. E. Fischer, P. A. Heiney, R. M. Strongin, L. Brard, and A. B. Smith III, in *Recent Advances in the Chemistry and Physics of Fullerenes and Related Materials*, edited by R. S. Ruoff and K. M. Kadish (The Electrochemical Society, Pennington, NJ, 1995), Vol. 2, p. 791.

[11] D. A. Neumann, J. E. Fischer, J. R. D. Copley, P. A. Heiney, J. J. Rush, R. M. Strongin, L. Brard, and A. B. Smith III, in *Science and Technology of Fullerene Materials*, edited by P. Bernier, T. W. Ebbesen, D. S. Bethune, R. M. Metzger, L. Y. Chiang, and J. W. Mintmire, MRS Symposia Proceedings No. 359 (Materials Research Society, Pittsburgh, 1995), p. 537.

[12] A. Cheng and M. L. Klein, J. Chem. Soc. Faraday Trans. **90**, 253 (1994).

[13] C. Meingast, G. Roth, M. M. Kappes, R. H. Michel, C. Stoermer L. Brard, P. A. Heiney, J. E. Fischer, A. B. Smith III, and R. M. Strongin, in *Physics and Chemistry of Fullerenes and Derivatives*, edited by H. Kuzmany, J. Fink, M. Mehring, and S. Roth (World Scientific, Singapore, 1995).

[14] K. M. Creegan, J. L. Robbins, J. M. Millar, R. D. Sherwood, P. J. Tindall, D. M. Cox, A. B. Smith III, J. P. McCauley, D. R. Jones, and R. T. Gallagher, J. Am. Chem. Soc. **114**, 1103 (1992); R. D. Beck *et al.*, J. Chem. Phys. **101**, 3243 (1994).

[15] R. H. Michel, H. Schreiber, R. Gierden, F. Hennrich, J. Rockenberger, R. D. Beck, and M. M. Kappes, Ber. Bunsenges. Phys. Chem. **98**, 975 (1994).

[16] In the low-temperature phase of $C_{60}O[Fe(C_5H_5)_2]_2$, the $C_{60}O$ molecules are ordered, which makes it possible to accurately determine both the C-O and bridged C-C bond lengths [G. Roth *et al.* (unpublished)].

[17] A. B. Smith III, H. Tokuyama, R. M. Strongin, G. T. Furst, and

W. J. Romanow, J. Am. Chem. Soc. **117**, 9359 (1995).
[18] S. Lebedkin, S. Ballenweg, J. Gross, R. Taylor, and W. Krätschmer, Tetrahedron Lett. **36**, 13 (1995).
[19] F. Hennrich, Diplom thesis, Universität Karlsruhe, 1995.
[20] C. Meingast, F. Gugenberger, R. Heid, P. Adelmann, M. Braun, H. Wühl, M. Haluska, and H. Kuzmany, in *Electronic Properties of Fullerenes*, edited by H. Kuzmany, J. Fink, M. Mehring, and S. Roth (World Scientific, Singapore, 1993).
[21] J. R. D. Copley, D. A. Neumann, R. L. Cappelletti, and W. A. Kamitakahara, J. Phys. Chem. Solids **53**, 1353 (1992).
[22] B. Renker, F. Gompf, R. Heid, P. Adelmann, A. Heiming, W. Reichardt, G. Roth, H. Schober, and H. Rietschel, Z. Phys. B **90**, 325 (1993).
[23] There are 6 octahedral and 8 tetrahedral sites around each molecule. The octahedral sites are all equivalent, whereas there are two different kinds of tetrahedral sites, TET1 and TET2, of which there are 6 and 2, respectively. For $C_{60}O$, we find 6 ''excellent'' (TET1) and 18 ''good'' ($2\times$OCT$+3\times$TET2) positions for the pentagon orientation. This is significantly better than the 6 ''good'' (OCT) and 12 ''fair'' ($2\times$TET1) positions for the hexagon orientation and, thus, favors the pentagon orientation.